Elsevier Editorial System(tm) for Applied Surface Science
Manuscript Draft

Manuscript Number: APSUSC-D-15-03031R1

Title: Metallization and stiffness of the Li-intercalated MoS2 bilayer

Article Type: Full Length Article

Keywords: Layered systems; MoS2; Density functional calculations; Electronic band structure; Stiffness

Corresponding Author: Prof. I.N. Yakovkin,

Corresponding Author's Institution: Institute of Physics

First Author: Nataliia V Petrova, Dr.

Order of Authors: Nataliia V Petrova, Dr.; I.N. Yakovkin; Dagou A Zeze, Dr.

Cover Letter

Dear Editors,

The paper has been amended accordingly to Reviewers' comments. All raised points have been carefully considered and addressed. As a result, the paper, to our view, has become better focused, i.e. significantly improved – many thanks to the referees.

Sincerely,

I.N. Yakovkin

***Highlights (for review)**

►Adsorbed or intercalated Li monolayer makes the MoS_2 surface metallic ► Increasing density of adsorbed Li leads to the nonmetal-to-metal transition in the layer ► Lithium inserted into MoS_2 bilayers increases the interlayer interaction

Graphical Abstract (for review)

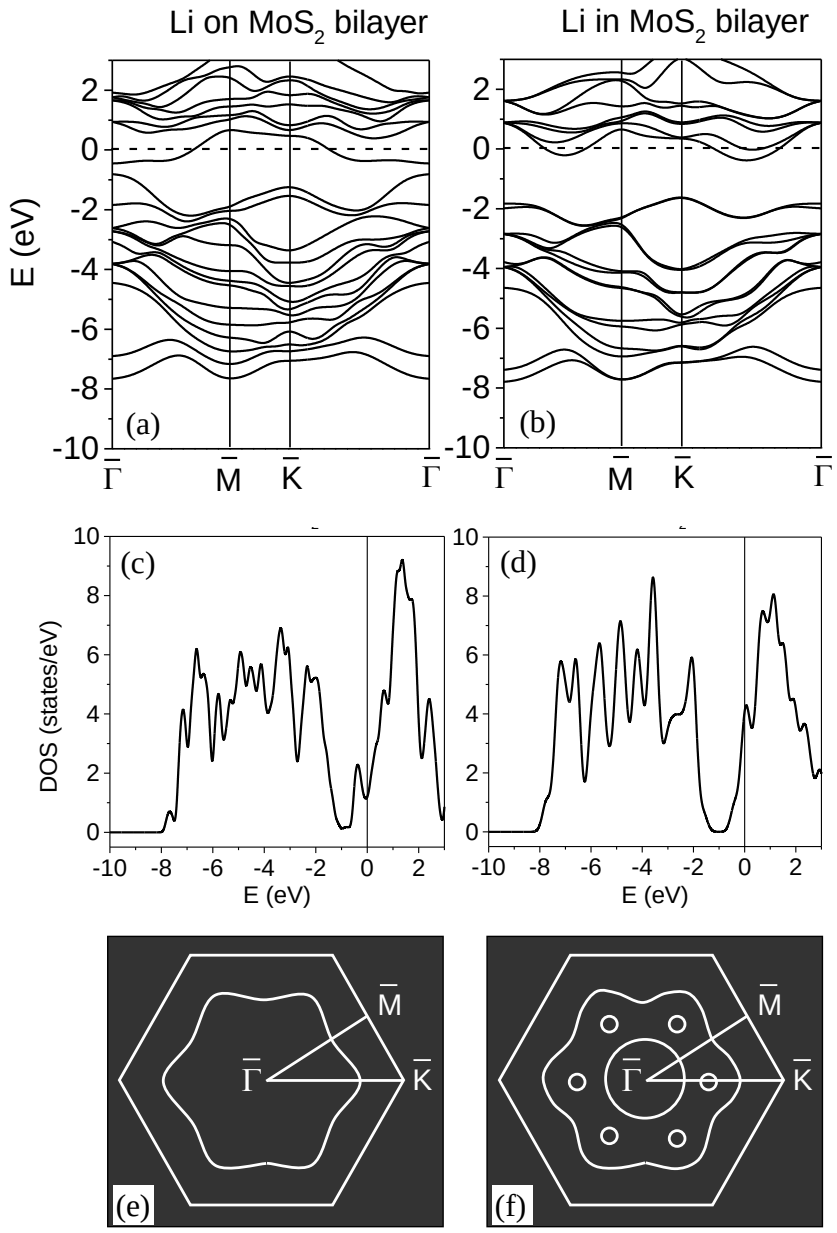

The band structures, DOS, and Fermi surfaces for the MoS_2 bilayer with adsorbed (a,c,e) and intercalated (b,d,f) Li (1×1) layer.

To Reviewer #1:

"1. The authors showed the frequencies of phonon modes at Gamma point. In Fig. 6 and Fig. 7, phonon densities of states and phonon band structures are also indicated. What's the relationship of them with the topic "Metallization and stiffness of the Li-intercalated MoS_2 bilayer"? It seems there is no words in abstract about this part, either in conclusion. I suggest the authors should add further explanation on this point."

- We have to confess that the relationship of the phonon frequencies at Gamma with the topic of the paper is only marginal, and therefore have canceled Table 1, Fig. 6 and Fig. 7 (with the related text), as advised. To our view, as a result, the paper has become more focused.

"2. Did the authors consider the van der Waals interactions in their calculations? This is important to study the interlayer interaction in MoS_2 bilayer."

- The issue of the role of vdW interactions between adjacent layers in inherently layered systems like graphite (or several-layer graphene) and MoS_2 has a long history – and has not been finally solved yet. While it is generally believed that the interlayer interaction should be attributed to vdW interaction (just because of a negligible overlap of wave functions or electron densities of adjacent layers) – in fact this overlap strongly depends on the adopted approximation for the exchange-correlation potential, as it was demonstrated for MoS_2 layers in Ref. [11] (I.N. Yakovkin, Surf. Rev. Lett. 21 (2014) 1450039). In particular, while in GGA the overlap is negligible indeed, in LDA it is significant. Accordingly, there is a number of examples when GGA does not give any bonding, while LDA provides realistic estimates, consistent with experiment. Then, to obtain any interlayer interaction using GGA, the inclusion of vdW corrections to the functional is mandatory, while within LDA the interaction appears reasonable even without any additives (as shown for MoS_2 in [11]). Phonon bands, calculated for MoS_2 monolayer and bilayer within LDA, are consistent with Raman spectra, thus further indicating the capability of LDA to correctly describe interactions in the layered system, including the interlayer interactions usually attributed to van der Waals forces. This unexpected property of LDA is well known and has been usually attributed to a fortuitous cancellation of errors in the exchange-correlation functional, nonetheless, the agreement of many LDA-calculated values with experiment is remarkable.

Of course, within LDA, one cannot achieve a "chemical accuracy" of the estimates of the interlayer interaction, but for the purposes of the present study of the role of Li intercalation, it is important to use the same approximation for both (pristine and Li-intercalated) systems, and here LDA is a good choice. It should be noted in this regard that, rigorously speaking, vdW description

is valid until wave functions of species do not overlap – otherwise, the exchange interaction must be considered instead.

Hence, though we do recognize the importance of vdW interaction between MoS_2 layers and appreciate recent efforts in development of novel vdW functionals, we believe that for the purposes of present comparative study of the influence of Li intercalation on the interlayer interaction LDA is adequate. We add corresponding explanations to the text ("Methodology", p. 4) and related references ([40-47]), as advised.

Metallization and stiffness of the Li-intercalated MoS_2 bilayer

N.V. Petrova,[1] I.N. Yakovkin,[1*] and D.A. Zeze[2]

[1] *Institute of Physics of National Academy of Sciences of Ukraine, Prospect Nauki 46, Kiev 03028, Ukraine*

[2] *School of Engineering & Computing Sciences, Durham University, Durham DH1 3LE, United Kingdom*

Performed density-functional theory (DFT) calculations have shown that the Li adsorption on the MoS_2 (0001) surface, as well as Li intercalation into the space between MoS_2 layers, transforms the semiconductor band structure of MoS_2 into metallic. For the $(\sqrt{3}\times\sqrt{3})$ – R30° Li layer, the band structures of the MoS_2 bilayer with adsorbed and intercalated Li are very similar, while for higher Li concentrations, the character of metallization for the adsorbed layer substantially differs from that of the MoS_2 – Li – MoS_2 layered system. In particular, for the adsorbed (1×1) Li monolayer, the increased density of the layer leads to the nonmetal-to-metal transition, which is evident from the appearance of the band crossing E_F with an upward dispersion, pertinent to simple metals. It has been demonstrated that intercalated Li substantially increases the interlayer interaction in MoS_2. Specifically, the estimated 0.12 eV energy of the interlayer interaction in the MoS_2 bilayer increases to 0.60 eV. This result is also consistent with results of earlier DFT calculations and available experimental results for alkali-intercalated graphene layers, which have demonstrated a substantial increase in the stiffness due to intercalation of alkalis.

Keywords: Layered systems; MoS_2; Density functional calculations; Electronic band structure; Stiffness

PACS: 68.47.Fg; 73.20.At; 73.22.-f

* Corresponding author. Email: yakov@iop.kiev.ua

1. Introduction

Layered systems have special properties which make them very promising in various applications such as nanoelectronics and catalysis [1-6]. Several transition-metal dichalcogenides exhibit a transformation from indirect to direct band gap semiconductors as they are thinned down to a single monolayer. For example, a MoS_2 monolayer exhibits a dramatic increase in luminescence quantum efficiency compared to the bulk material [7-9]. The explanation of these phenomena was found with the help of the band structure calculations [8-11], which have revealed, in agreement with recent High-Resolution Ultraviolet Photoelectron Spectroscopy (HRUPS) study [12] an increase of the gap width and a transformation of the band gap from indirect for the bulk MoS_2 to direct for monolayer. It should also be noted also that the symmetry of the monolayer (D_{3h} point group) differs from that of the bulk (D_{6h}) by virtue of the absence of the inversion symmetry, which indicates possible k-dependent spin-orbital splitting of the bands (Rashba effect) [11-13]. The density-functional theory calculations of the piezoelectric coefficients of MoS_2, $MoSe_2$, $MoTe_2$, and some other relative monolayers have revealed a strong piezoelectric coupling, which enables the development of new electronic components for nanoscale devices based on the piezoelectric effect. [14]

The electronic, catalytic, and mechanical properties of layered systems can be modified and further improved by intercalating alkalis [9,15-20]. The most prominent example, perhaps, is the appearance of superconductivity of alkali doped graphite [21-23]. By increasing the alkali metal concentration, the transition temperature can be increased up to 5 K in C_2Na [23]. The Li intercalated graphite, as well as MoS_2, is also a promising compound material for Li ion rechargeable batteries. Therefore it is not surprising that studies of these systems have a long history [15,17,20]. With increasing the alkali doping, the graphene-based systems become "more metallic", i.e., the density of states (DOS) at Fermi level significantly increases [17-19]. In particular, DFT calculations for bulk C_6Li, Li-intercalated free-standing bilayer graphene, and Li-intercalated bilayer and trilayer graphene on SiC(0001) have demonstrated a large enhancement of the charge carrier density caused by Li intercalation [19,24].

The alkali-doped MoS_2, in turn, is particularly important due to the transition from semiconducting to metallic state (non-metal-to-metal transition), as recently found in combined experimental (HRUPS) and theoretical (DFT) study of Na doped MoS_2 (0001) surface [25]. It was concluded that deposited Na stayed on the surface, i.e., did not penetrate underneath the surface monolayer. This suggestion was argued by results of a similar study of K intercalated in the interlayer gap of MoS_2 crystal [9]. Specifically, it was shown that K expands the interlayer spacing while simultaneously doping electrons into the conduction band. Consequently, the system became

metallic (with electronic pockets of the Fermi surface). Nonetheless, the authors proposed that K intercalation creates an isolated monolayer at the surface of a bulk MoS_2 crystal.

Small Li atoms are expected to penetrate into the interlayer space (presumably, through S-vacancies in the surface layer, similarly to H atoms [26]) more readily than larger Na and K. Note that Li can be intercalated into bilayer graphene, without any pronounced distortion of the structure [27]. The DFT calculations of Young's modulus for Li-intercalated bilayer and trilayer graphene have shown that the intercalation increases the intrinsic stiffness. [24]. Similar results have also been reported for K-intercalated graphite systems [28]. In the presence of K, the in-plane lattice constant remains similar to that of graphite, while the out-of-plane lattice constant increases. Therefore, it was suggested [28] that the components of the elastic modulus associated with the deformation of the atomic plane (C_{11} and C_{66}) would change only slightly while those associated with the deformation normal to the atomic plane (C_{33} and C_{44}) should increase significantly, resulting in an overall enhancement of Young's modulus.

Recently, Bertolazzi et al. [29] performed the experimental measurements on the stiffness and breaking strength of monolayer MoS_2 by using an atomic force microscope tip to deform the monolayer MoS_2 placed on a prepatterned SiO_2 substrate. They determined an effective Young's modulus of monolayer MoS_2 of 270 GPa, which significantly exceeds the Young's modulus of the bulk MoS_2 of 220 GPa. An even higher value (330 GPa) for the mean Young's modulus was obtained in a similar study of mechanical properties of freely suspended MoS_2 nanosheets [30].

It should be noted that estimates of Young's modulus for layered systems from atomistic calculations are not always straightforward. For example, the supercell stress as output directly by ABINIT [31] is the stress averaged over the supercell volume, which depends on the size of the chosen supercell. Accordingly, Li et al. [32] renormalized the calculated stress for a monolayer by a factor of Z / h, where Z is the vacuum distance and h is the interlayer distance in the bulk MoS_2. To overcome the problem of the biased determination of the effective thickness of a monolayer [29,32], various approximations were adopted [33-35]. Thus, to estimate the elastic bending modulus of single-layer MoS_2, Jiang et al. [35] derived an analytic formula based on an empirical interaction potential.

Another possibility to estimate the Young modulus for a single monolayer or bilayer in DFT calculations consists of applying of tensile strains followed by calculations of the stress produced. Thus, in Ref. [36], the supercell was deformed along the high symmetry direction in small strain increments and the in-plane supercell vector normal to the applied strain was allowed to relax in order to account for the Poisson's contraction. Consistently with the hexagonal symmetry in the basal plane, the Young's moduli for MoS_2 monolayer, obtained for armchair and zigzag loading direction, were found to be virtually identical.

In the present paper the electronic band structure, interlayer interaction, and elastic properties of Li-intercalated MoS_2 bilayer are studied by means of DFT calculations. We demonstrate that Li monolayer inserted into the MoS_2 bilayer leads to a metallic state of the system and significantly increases the interlayer interaction.

2. Methodology

The DFT semirelativistic calculations of total energies and related favorable structures were carried out with the ABINIT code [31] using the Troullier-Martins [37] norm-conserving pseudopotentials and local density approximation (LDA) with GTH [38] exchange-correlation functional. The periodicity in the direction normal to the surface was introduced by using the repeated-slab model. The 12×12×1 Monkhorst-Pack [39] lattice of k-points (including Γ point) and the energy cutoff of 24 Ha provided the 10^{-4} Ha convergence of total energy. A standard optimization was terminated when the forces on atoms were below 0.02 eV/Å, which provided the determination of atomic positions with an accuracy of ~0.01 Å. The thickness of the vacuum gap was about 10 Å.

The choice of LDA was dictated by its ability to estimate binding energies and equilibrium separations for layered systems better than commonly used GGA functionals [40-42]. It has been found also [11] that LDA provides an adequate description of the fundamental band gap in the MoS_2 monolayer as well as of the interlayer interaction in the bulk MoS_2. In particular, phonon bands, calculated for MoS_2 monolayer and bilayer within LDA, are consistent with Raman spectra, thus indicating the capability of LDA to describe the interlayer interactions usually attributed to van der Waals forces. This unexpected property of LDA is well known [40-44] and is usually attributed to a fortuitous cancellation of errors in the exchange-correlation functional, nonetheless, the agreement of many LDA-calculated values with experiment is remarkable.

The nonlocal corrections to GGA-type density functionals [40,43-47], which correctly reproduce the asymptotic van der Waals tail of the binding energy curve, have little impact on the charge distribution at the interface [42], so that, for the graphene/metal systems, the obtained results are qualitatively similar to the LDA results [40-42]. Hence, though we do recognize the importance of the van der Waals interaction between MoS_2 layers, we believe that for the purposes of present comparative study of the influence of Li intercalation on the electronic structure of MoS_2 and interlayer interaction the LDA is sufficient and can provide an adequate description.

The lattice constants of the bulk MoS_2, obtained after a net structural optimization within LDA, were a = 3.15 Å and c = 12.09 Å, consistent with the experimental lattice parameters a = 3.15 Å and c = 12.32 Å, respectively. The length of the Mo – S bond was of 2.406 Å. For the bilayer (Fig.

1a), the interlayer spacing, defined as the distance between Mo planes, was of the order of 6.04 Å (so that the distance between neighboring S planes was ~ 2.90 Å).

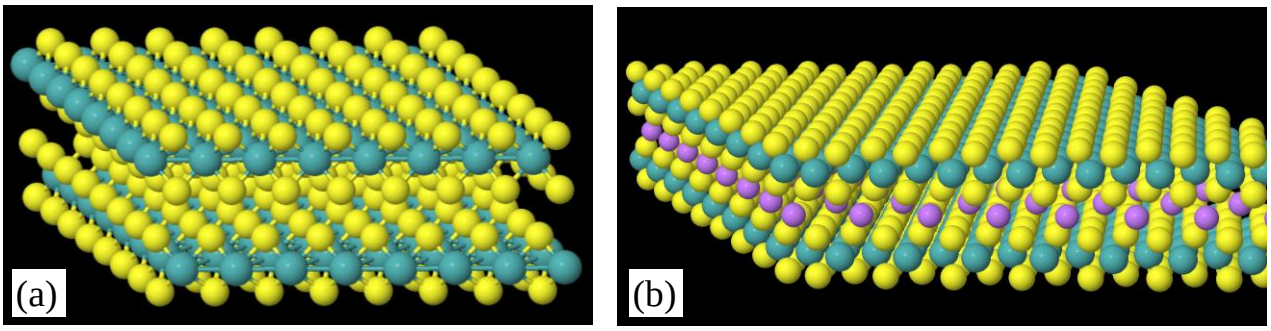

Fig. 1. The MoS_2 bilayer (a) and MoS_2 – Li – MoS_2 system (b). Mo atoms are blue, S yellow, and Li pink.

3. Results and discussion

3.1. Li (√3×√3) – R30° on MoS_2

Li adsorbed on graphene or intercalated in graphene bilayers tend to form the (√3×√3) – R30° structure [19,24]. Therefore it can be expected that this structure with the stoichiometric Li coverage θ = 1/3 will also readily form in the case of the MoS_2 (Fig. 2a). To determine the most favorable adsorption sites on the surface, we have performed calculations of binding energies for various symmetric positions of adsorbed Li in the surface cell. As expected, both in the (√3×√3) – R30° and (1×1) structures, Li adatoms tend to occupy 3-fold hollow sites. In the (√3×√3) – R30° structure of the MoS_2 – Li – MoS_2 layered system (Fig. 2b), Li atoms also prefer 3-fold sites. In contrast to intercalated hydrogen [48], Li does not reconstruct the MoS_2 bilayer, which retains the central symmetry pertinent to the bulk.

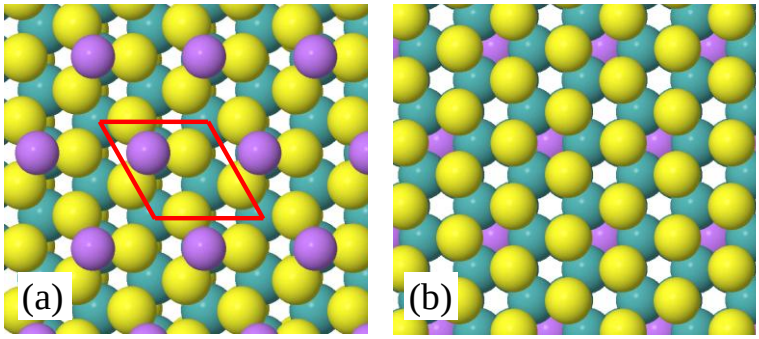

Fig. 2. The (√3×√3) – R30° structure of Li adsorbed on the MoS_2 surface (a) and inserted in the MoS_2 bilayer (b). Mo atoms are blue, S yellow, and Li pink.

The MoS_2 is an indirect gap semiconductor [2-4]. For the MoS_2 bilayer, the bands become slightly flatter compared to bulk, so that the gap increases [11]. In contrast, the bilayer with adsorbed or intercalated Li (√3×√3) – R30° layer is metallic, as it is evident from the band structure and DOS (Fig. 3). The metallicity of the both layered systems follows from the crossing of the bands by Fermi level and non-zero density of states at this energy. It should be noted that the band structures for adsorbed and intercalated Li appear quite similar (c.f. Fig. 3 a and b), and the difference in DOS at E_F is also insignificant (Fig. 3c). Hence, for moderate concentrations of Li, it must be difficult to distinguish between the cases of Li adsorption and intercalation by means of HRUPS, as it was suggested for K/MoS_2 (0001) [9].

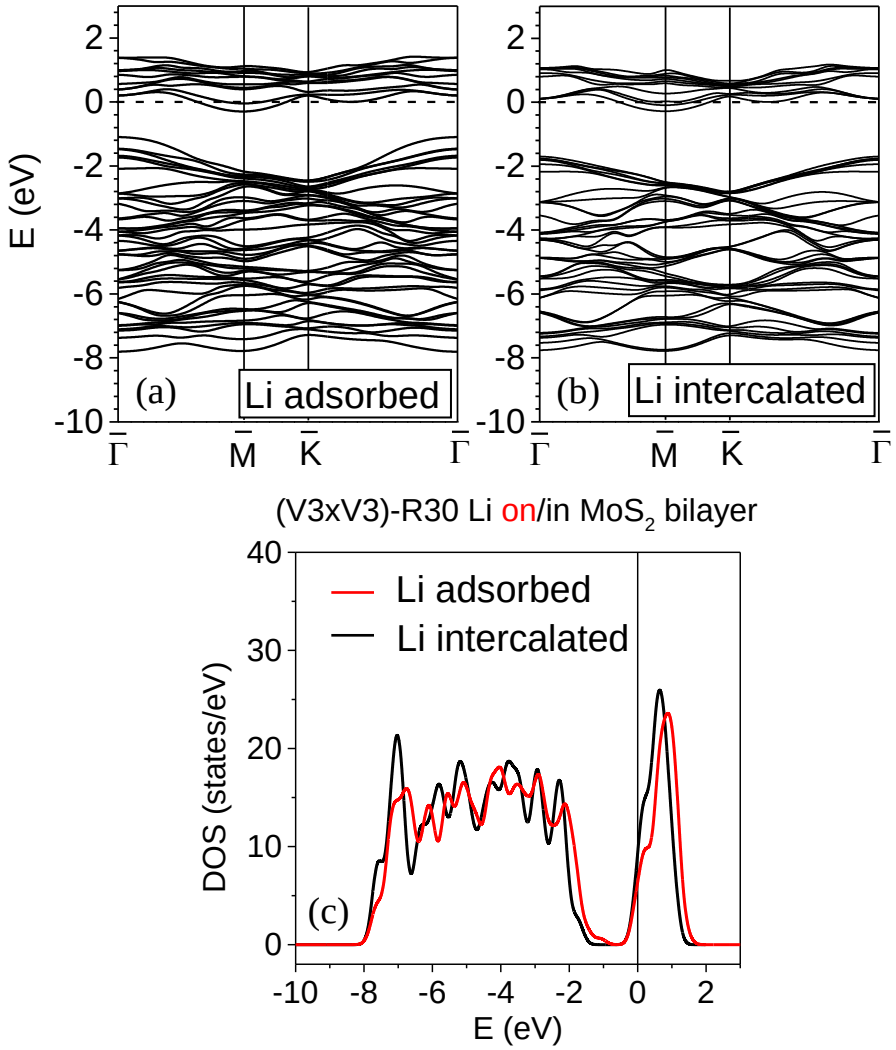

Fig. 3. The band structure (a,b) and DOS (c) for the MoS_2 bilayer with adsorbed (a) and intercalated (b) Li ($\sqrt{3}\times\sqrt{3}$) – R30° layer.

In contrast, for a complete Li monolayer (having the (1×1) structure), the difference of band structures for adsorbed and intercalated Li is evident (Fig. 4 a,b). In particular, while for the intercalated Li the changes of the bands in vicinity of E_F due to increasing amount of Li are only minor, the increase of the density of the adsorbed Li layer results in a drastic transformation of the bands crossing E_F. The most important here is the appearance of the band with an upward dispersion, crossing E_F approximately at the middle of BZ along the Γ – K line. Although this band at Γ could hardly be approximated by a parabola, the upward dispersion unambiguously indicates the metallization of the adsorbed Li layer. In other words, the increase of the concentration of Li on the MoS_2(0001) surface leads to the nonmetal-to-metal transition (NMT) in the adsorbed layer (for reviews of NMT in adsorbed films see, e.g., [49-51]). Hence, it can be expected that for sufficiently high Li concentrations, the absence of intercalation indeed can be concluded from HRUPS by dispersion of the band(s) crossing E_F, as observed for Na/MoS_2(0001) [25].

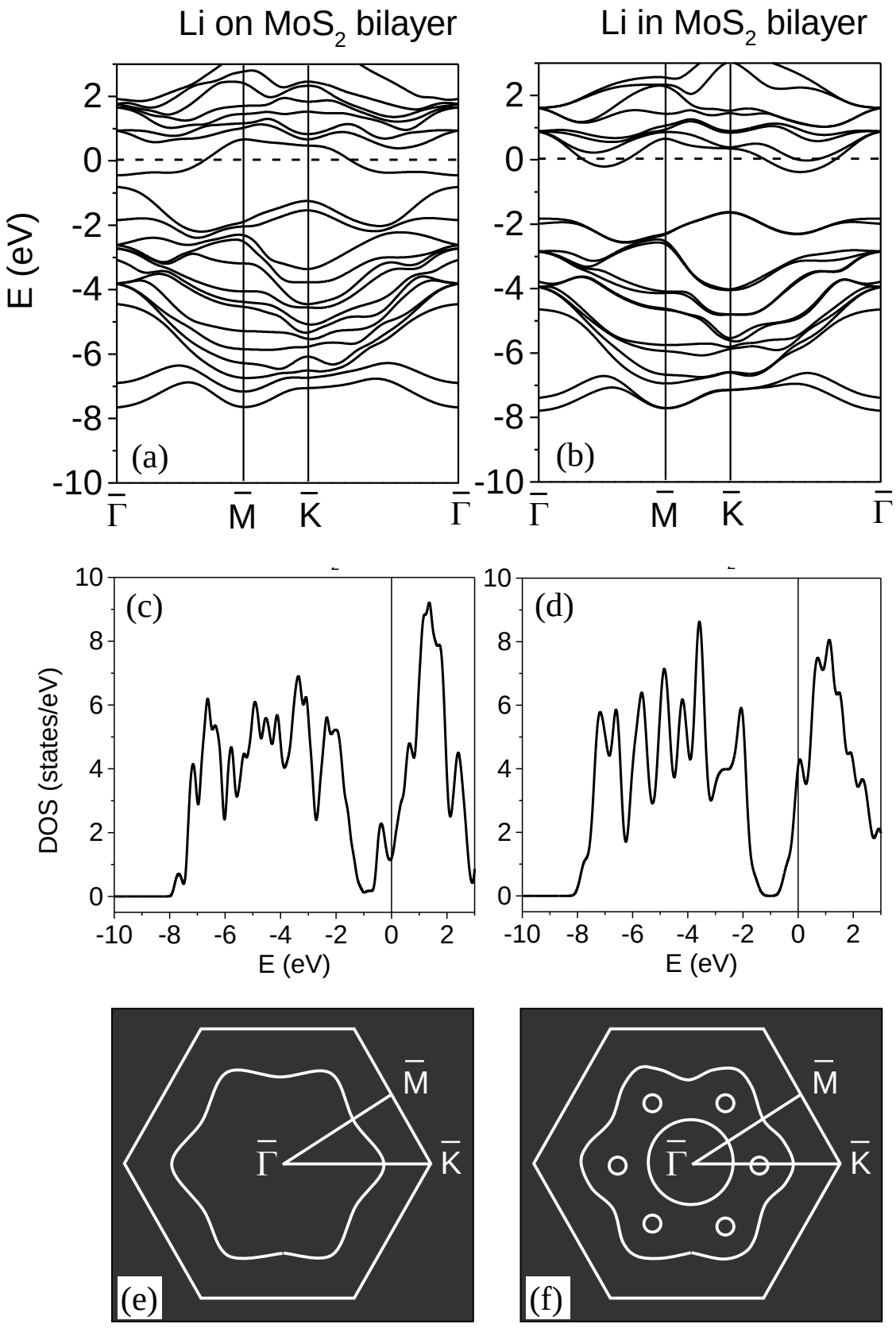

Fig. 4. The band structures, DOS, and Fermi surfaces for the MoS_2 bilayer with adsorbed (a,c,e) and intercalated (b,d,f) Li (1×1) layer.

The difference of electronic structures of the MoS_2 bilayers with adsorbed and intercalated Li(1×1) sheets can be also seen in the densities of states (Fig. 4 c,d) at E_F and Fermi surfaces (Fig. 4 e,f). While for the adsorbed Li the DOS at E_F indicates a metallic state of the Li monolayer, the intercalation leads to the metallization of the net system and to a significant rise of the DOS at Fermi energy. Namely, for the intercalated Li monolayer, the "degree of metallization" [25] is approximately twice that of the adsorbed Li.

The difference in the Fermi surfaces can be described as an appearance of additional features pertinent to intercalated Li but which are absent for the bilayer with adsorbed Li. Indeed, there is only one band crossing E_F (both along Γ – K and Γ – M lines) in the case of adsorbed layer (Fig. 4 a), while for intercalated Li the number of such bands increases to 3 (one of them just touching E_F) (Fig. 4 b). Accordingly, these bands give rise to additional sheets of the Fermi surface (c.f. Fig. 4 e and f).

3.2. Interlayer interaction

The binding energy between MoS_2 layers in the bilayer, estimated as $E_b = E_{Bilayer} - 2E_{Monolayer}$, is found to be of 0.12 eV. This value corresponds to the depth of the potential well (0.116 eV) in the dependence of the energy of interlayer interaction on the distance between layers shown in Fig. 5a. Due to inserted Li, the binding energy between the layers increases dramatically. The dependence of the energy of the interlayer interaction on the distance between layers, shown in Fig. 5b, was obtained by stepwise increasing the distance between the MoS_2 and MoS_2 – Li layers, with structural optimization at each step keeping the Mo – Mo distance *d* fixed. Due to the intercalated

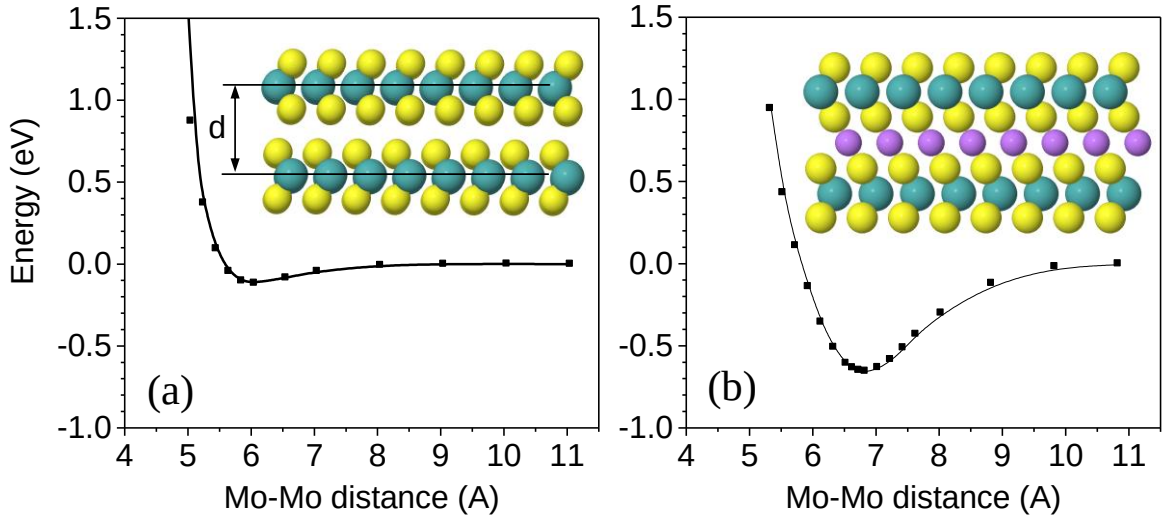

Fig. 5. The dependence of the energy of interlayer interaction on the distance between the MoS_2 layers for the bilayer (a) and the MoS_2 – Li – MoS_2 system (b).

Li layer, the depth of the potential well increases to 0.65 eV, which is indicative of a significant increase in the interlayer interaction.

To estimate the changes of the stiffness due to Li intercalation, we have calculated the response of the system to the strain normal to the surface (that is, along z coordinate). The induced force is found to be 6.4 meV/Å for the bilayer and 12 meV/Å for the Li intercalated bilayer. This change of the force resembles the stress induced by the strain (through the generalized Hook's law), but is not equivalent to the latter (usually defined as pressure) and does not imply the applicability of the continuous media model.

4. Conclusion

Performed DFT calculations have shown that the Li adsorption on the MoS_2 (0001) surface, as well as intercalation into the space between MoS_2 layers, transforms a semiconductor band structure of MoS_2 into metallic. For the $(\sqrt{3}\times\sqrt{3}) - R30°$ Li layer, the band structures of the MoS_2 bilayer with adsorbed and intercalated Li are very similar. In both cases, the metallic state results from the bands with a downward dispersion crossing E_F. For higher Li concentrations, the character of metallization for the adsorbed layer substantially differs from that of the $MoS_2 - Li - MoS_2$ layered system. In particular, for the adsorbed (1×1) Li monolayer, the increased density of the layer leads to the nonmetal-to-metal transition. The metallization of the Li monolayer is clearly evidenced by the appearance of the band crossing E_F with an upward dispersion, pertinent to simple metals. It can therefore be expected that for sufficiently high Li concentrations, the absence of intercalation can indeed be concluded from HRUPS, as observed for the $Na/MoS_2(0001)$ [25].

In contrast to intercalated hydrogen [48], Li does not reconstruct the MoS_2 bilayer, which retains the central symmetry pertinent to the bulk. Nonetheless, Lithium atoms, intercalated into the space between MoS_2 layers, substantially increase the interlayer interaction. Specifically, the estimated 0.12 eV energy of the interlayer interaction in the MoS_2 bilayer increases to 0.60 eV. This result is also consistent with the results of DFT calculations and experimental results available in the literature for alkali-intercalated graphene layers [17-24], which have demonstrated substantial increase in the stiffness due to the intercalation of alkalis.

Acknowledgments. The financial support from the European Union through FUNPROB (PIRSES-GA-2010-269169) is gratefully acknowledged. We thank Durham University for provided High Performance Computer Facilities.

References

1. K.S. Novoselov, D. Jiang, F. Schedin, T.J. Booth, V.V. Khotkevich, S.V. Morozov, A.K. Geim, Proc. Natl. Acad. Sci. USA 102 (2005) 10451.
2. T.S. Li, G.L. Galli, J. Phys. Chem. C 111 (2007) 16192.
3. S. Lebegue, O. Eriksson, Phys. Rev. B 79 (2009) 115409.
4. B. Radisavljevic, A. Radenovic, J. Brivio, V. Giacometti, A. Kis, Nat. Nanotechnol. 6 (2011) 147.
5. V. P. Santos, B. van der Linden, A. Chojecki, G. Budroni, S. Corthals, H. Shibata, G. R. Meima, F. Kapteijn, M. Makkee, J. Gascon, ACS Catal. 3 (2013) 1634.
6. A. Andersen, S. M. Kathmann, M. A. Lilga, K. O. Albrecht, R. T. Hallen, D. Mei, J. Phys. Chem. C 115 (2011) 9025.
7. K.F. Mak, C. Lee, J. Hone, J. Shan, T.F. Heinz, Phys. Rev. Lett. 105 (2010) 136805.
8. A. Splendiani, L. Sun, Y. Zhang, T. Li, J. Kim, C.-Y. Chim, G. Galli, F. Wang, Nano Lett. 10 (2010) 1271.
9. T. Eknapakul, P. D. C. King, M. Asakawa, P. Buaphet, R.-H. He, S.-K. Mo, H. Takagi, K. M. Shen, F. Baumberger, T. Sasagawa, S. Jungthawan, W. Meevasana, Nano Lett. 14 (2014) 1312.
10. T. Cheiwchanchamnangij, W.R.L. Lambrecht, Phys. Rev. B 85 (2012) 205302.
11. I.N. Yakovkin, Surf. Rev. Lett. 21 (2014) 1450039.
12. T. Komesu, D. Le, Q. Ma, E. F. Schwier, Y. Kojima, M. Zheng, H. Iwasawa, K. Shimada, M. Taniguchi, L. Bartels, T. Rahman, P. A. Dowben, J. Phys.: Condens. Matter 26 (2014) 455501.
13. Di Xiao, G.-B. Liu, W. Feng, X. Xu, W. Yao, Phys. Rev. Lett. 108 (2012) 196802.
14. K.-A.N. Duerloo, M.T. Ong, E.J. Reed, J. Phys. Chem. Lett. 3 (19) (2012) 2871.
15. K.T. Park, J. Kong, Topics in Catalysis 18 (2002) 175.
16. M. Kamaratos, D. Vlachos, C.A. Papageorgopoulos, J. Phys. Condens. Matter 5 (2014) 535.
17. N.A.W. Holzwarth, S. Rabii, L.A. Girifalco, Phys. Rev. B 18 (1978) 5190.
18. N.A.W. Holzwarth, S.G. Louie, S. Rabii, Phys. Rev. B 30 (1984) 2219.
19. C. Hartwigsen, W. Witschel, E. Spohr, Phys. Rev. B 55 (1997) 4953.
20. K. Sugawara, K. Kanetani, T. Sato, T. Takahashi, AIP Advances 1 (2011) 022103.
21. G. Csányi, P.B. Littlewood, A.H. Nevidomskyy, Ch.J. Pickard, B.D. Simons, Nature Physics 1 (2005) 42.
22. Y. Koike, H. Suemetsu, K. Higuchi, S. Tanuma, Physica *B+C* 99 (1980) 503.
23. I.T. Belash, A.D. Bronnikov, O.V. Zharikov, A.V. Palnichenko, Solid State Commun. 64 (1987) 1445.
24. T.P. Kaloni, Y.C. Cheng, M. Upadhyay Kahaly, U. Schwingenschlögl, Chem. Phys. Lett. 534 (2012) 29.

25. T. Komesu, Duy Le, Xin Zhang, Q. Ma, E.F. Schwier, Y. Kojima, M. Zheng, H. Iwasawa, K. Shimada, M. Taniguchi, L. Bartels, T.S. Rahman, P.A. Dowben, Applied Physics Letters 105, (2014) 241602.
26. E.W. Keong Koh, C.H. Chiu, Y.K. Lim, Y.-W. Zhang, H. Pan, Int. J. Hydrogen Energy 37 (19) (2012) 14323.
27. S. Watcharinyanon, L.I. Johansson, A.A. Zakharov, C. Virojanadara, Surf. Sci. 606 (2012) 401.
28. T.P. Kaloni, M. Upadhyay Kahaly, Y.C. Cheng, U. Schwingenschlögl, Europhysics Letters 98 (2012) 67003.
29. S. Bertolazzi, J. Brivio, A. Kis, ACS Nano 5 (2011) 9703.
30. A. Castellanos-Gomez, M. Poot, G.A. Steele, H.S.J. van der Zant, N. Agrait, G. Rubio-Bollinger, Adv. Mater. 24 (2012) 772.
31. X. Gonze, J.-M. Beuken, R. Caracas, F. Detraux, M. Fuchs, G.-M. Rignanese, L. Sindic, M. Verstraete, G. Zerah, F. Jollet, M. Torrent, A. Roy, M. Mikami, Ph. Ghosez, J.-Y. Raty, D.C. Allan, Comput. Mat. Sci. 25 (2002) 478.
32. J. Li, N.V. Medhekar, V.B. Shenoy, J. Phys. Chem. C 117 (30) (2013) 15842.
33. M. Arroyo, T. Belytschko, Phys. Rev. B 69 (2004) 115415.
34. L. Wang, Q. Zhang, J.Z. Liu, Q. Jiang, Phys. Rev. Lett. 95 (2005) 105501.
35. J.-Wu Jiang, Z. Qi, H. S. Park, T. Rabczuk, Nanotechnology 24 (2013) 435705.
36. Q. Yue, J. Kang, Z. Shao, X. Zhang, S. Chang, G. Wang, S. Qin, J. Li, Phys. Lett. A 376 (2012) 1166.
37. N. Troullier, J.L. Martins, Phys. Rev. B 43 (1991) 1993.
38. S. Goedecker, M. Teter, J. Hutter, Phys. Rev. B 54 (1996) 1703.
39. H.J. Monkhorst, J.D. Pack, Phys. Rev. B 13 (1976) 5188.
40. P.A. Khomyakov, G. Giovannetti, P.C. Rusu, G. Brocks, J. van den Brink, P.J. Kelly, Phys. Rev. B 79 (2009) 195425.
41. P.J. Feibelman, Top. Catal. 53 (2010) 417.
42. R. Brako, D. Šokčević, P. Lazić, N. Atodiresei, New Journal of Physics 12 (2010) 113016.
43. J. Klimeš, A. Michaelides, J. Chem. Phys. 137 (2012) 120901.
44. P. L. Silvestrelli, A. Ambrosetti, J. Chem. Phys. 140 (2014) 124107.
45. S. Grimme, J. Comput. Chem. 25 (2004) 1463.
46. M. Dion, H. Rydberg, E. Schröder, D.C. Langreth, B.I. Lundqvist, Phys. Rev. Lett. 92 (2004) 246401.
47. T. Thonhauser, V.R. Cooper, S. Li, A. Puzder, P. Hyldgaard, D.C. Langreth, Phys. Rev. B 76 (2007) 125112.
48. I.N. Yakovkin, N.V. Petrova, Chem. Phys. 434 (2014) 20.
49. P.A. Dowben, Surf. Sci. Rep. 40 (2000) 151.

50. I.N. Yakovkin, Appl. Surf. Sci. 252 (2006) 6127; JNN 1 (2001) 357.
51. I.N. Yakovkin, Atomic Wires, in: *Encyclopedia of Nanoscience and Nanotechnology*, Edited by H.S. Nalwa, American Scientific Publishers (2004), Vol. 1, pp. 169-190.